Deuterium diffusion in silicon-doped diamondlike carbon films

E. Vainonen-Ahlgren,* T. Ahlgren, J. Likonen,† S. Lehto,† T. Sajavaara, W. Rydman, and J. Keinonen
Accelerator Laboratory, P.O. Box 43, FIN-00014 University of Helsinki, Finland

C. H. Wu
EFDA CSU, European Fusion Development Agreement Close Support Unit, Max-Planck-Institut für Plasmaphysik, Boltzmannstrasse 2 D-85748 Garching bei München, Germany
(Received 4 May 2000; published 9 January 2001)

Diffusion of deuterium in diamondlike carbon films with different Si contents deposited by a pulsed arc discharge method in deuterium atmosphere was studied. The concentration profiles of D were measured by secondary-ion-mass spectrometry and elastic-recoil-detection techniques. A model is proposed to describe the experimental depth profiles. Diffusion, detrapping, and trapping of D were taken into account in this model. Diffusion coefficients obtained for nontrapped D resulted in activation energies of 1.5 ± 0.2, 0.7 ± 0.2, 0.6 ± 0.2, and 1.2 ± 0.2 eV for samples containing 0, 6, 15, and 33 at.% of Si, respectively.

DOI: 10.1103/PhysRevB.63.045406 PACS number(s): 66.30.Jt, 61.72.Ss

I. INTRODUCTION

There is a growing interest in the synthesis and study of diamondlike carbon (DLC) films. Semiconducting diamond doped with different impurities is expected to have applications in temperature-resistant and high-performance electronic devices.[1,2] Properties of these devices are sensitive to hydrogen contamination acting as a passivator.[3,4] In the next-step fusion device, the International Thermonuclear Experimental Reactor, carbon fiber composites are interesting candidates for diverter armor materials. In the presence of plasma, redeposition of sputtered carbon particles and the formation of carbon based composite films will take place. The uptake and release of deuterium and tritium from the films will significantly affect the recycling of D and T fuel as well as tritium retention in the fusion device.

A decrease of the chemical sputtering by a factor of 2 to 3 in silicon-doped carbon[5] compared to pure carbon makes this material attractive for application in a fusion device. In addition, Si doping will decrease the baking temperature needed to remove impurities from surfaces. Si is also known to be a good oxygen getter and an impurity that increases thermal conductivity.[5]

Despite the fact that hydrogen diffusion in carbon based materials has been studied intensively,[6–8] the mechanism of the process is not well understood. Moreover, the different allotropic forms of carbon have totally different H diffusivities, i.e., no significant diffusion in crystalline diamond, but fast migration in graphite. The situation gets even more complicated if dopants are introduced into the carbon network.

Recent publications demonstrate that diffusion of hydrogen isotopes in different carbon based materials can be modeled using different approaches.[9,10] No unified model has yet been proposed that can explain experimental results of thermal treatment in different carbon materials. This paper continues our studies on the migration of hydrogen isotopes in carbon films.[11,12] To our knowledge, there are no systematic experimental data in the literature on the migration of deuterium in Si-doped carbon materials. In the current paper a model is proposed that describes the diffusion of hydrogen isotopes in DLC films and graphite, implanted and co-deposited films, and undoped and Si-doped coatings. A computationally efficient numerical method to solve the complicated diffusion and rate equation is also presented.

II. EXPERIMENT

The 500 to 800 nm thick DLC films were deposited onto crystalline Si wafers with pulsed cathodic arc discharge facilities of DIARC Technology Inc. (Finland). The cathodes were prepared by milling in an attritor type ball mill and mixing pure graphite (Lonza KS 44) and silicon (ground from Okmetic semiconductor grade wafers) powders that were further solidified by hot isostatic pressing technique. Details of the deposition procedure are described elsewhere.[11] A pure graphite cathode was used to produce films without Si.

Annealing was performed in a quartz-tube furnace (pressure below 2×10^{-4} Pa) at temperatures from 600 to 1100 °C. The annealing time varied from 1 to 24 h.

The mass density of the DLC films and Si content was investigated by Rutherford backscattering spectrometry with 2.4-MeV ^{4}He ions obtained from a 2.5-MV Van de Graaff accelerator of the University of Helsinki. Backscattered particles were detected with a 50-mm^2 active area silicon surface-barrier detector placed at a scattering angle of 170°. The spectra were analyzed by the GISA3.99 program.[13] The results of measurements showed that the Si content of different sample sets was 6, 15, and 33 at. %. The mass densities were found to be 2.4 g/cm^3 for the films without Si and with a Si content of 6 at. %, and 2.6 and 2.8 g/cm^3 for the films with Si contents of 15 and 33 at. %, respectively.

The time-of-flight elastic recoil detection analysis (TOF-ERDA) of elementary concentration profiles was performed with the 5-MV tandem accelerator EGP-10-II of the University of Helsinki. In the measurements, a 53-MeV beam of $^{127}I^{10+}$ ions was used. The detector angle was 40°, and the samples were tilted relative to the beam direction by 20°. The elementary concentrations were calculated using known geometry and SRIM-96 stopping powers[14,15] in energy-loss

calculations.[16] The amount of retained deuterium in the samples increased with Si concentration and was found to be 2.9, 3.0, 3.7, and 4.8 at. % for films with an Si content of 0, 6, 15, and 33 at. %, respectively.[22] The amounts of O and H impurities increased with the Si concentration from 0.1 at. % (no Si) up to 1–3 at. % (33 at. % Si).

The depth profiling of D atoms was also carried out by secondary-ion-mass spectrometry (SIMS) at the Technical Research Center of Finland using a double focusing magnetic sector SIMS (VG Ionex IX70S). The current of the 5-keV O_2^+ primary ions was typically 400 nA during depth profiling and the ion beam was raster scanned over an area of 270×430 μm^2. Crater wall effects were avoided by using a 10% electronic gate and 1-mm optical gate. The pressure inside the analysis chamber was 5×10^{-8} Pa during the analysis. The depth of the craters was measured by a profilometer (Dektak 3030ST). The uncertainty of the crater depth was estimated to be 8%. Data of TOF-ERDA measurements were used to normalize the D concentration obtained in SIMS experiments.

The analysis of surface morphology was performed with a Zeiss 962 digital scanning electron microscope equipped with a dispersive x-ray detector. The scanning electron microscopy measurements indicated the presence of microparticles at the film surface, and the average size was the smallest (0.3 μm) for the Si-free films and the largest (3 μm) for the Si content of 6 at. %. Particle size for the Si contents of 15 and 33 at. % was about 1.5 μm. The observed microparticles were most probably extracted by the arc discharge from the cathode material. Raman-scattering measurements revealed that no crystallization of Si precipitates took place.[17]

III. ANALYSES OF DATA

The model outlined in this paper is based on the assumption that in carbon based material hydrogen isotopes exist in two different states. Most of the hydrogen atoms are quite strongly bonded to nearby carbon or silicon atoms. Some amount of hydrogen atoms is assumed to be in a nonbonded state and can migrate in the substrate. These mobile atoms can be trapped by dangling bonds. This process is described by a trapping rate. The bonded hydrogen can in return be thermally activated and detrapped, described by a detrapping rate.

A. Diffusion model

The diffusion equation describing the migration, thermal detrapping, and retrapping of nontrapped deuterium, $C(x,t)$, is given as[10]

$$\frac{\partial C}{\partial t}=D_f\frac{\partial^2 C}{\partial x^2}+\Sigma_D C_t-\Sigma_T(T_d-C_t)C. \tag{1}$$

The equation for trapped deuterium, $C_t(x,t)$, is

$$\frac{\partial C_t}{\partial t}=-\Sigma_D C_t+\Sigma_T(T_d-C_t)C. \tag{2}$$

D_f is the diffusion coefficient for nontrapped deuterium, Σ_D and Σ_T are the detrapping and trapping rate constants, respectively, T_d is the density of traps, which can be depth dependent, x is the depth from the surface, and t is the diffusion time. The total deuterium concentration, C_{tot}, is the sum of the nontrapped and trapped atoms. The initial concentrations of nontrapped $C(x,0)$ and trapped deuterium $C_t(x,0)$ in the layer of thickness L are

$$C(x,0)=C_{tot}-T_d, \tag{3}$$

$$C_t(x,0)=T_d, \tag{4}$$

if $C_{tot}>T_d$, and

$$C(x,0)=0, \tag{5}$$

$$C_t(x,0)=C_{tot}, \tag{6}$$

if $C_{tot}\leqslant T_d$. The boundary condition for Eq. (1) at the surface, where atomic hydrogen is thermally desorbed, is

$$D_f\frac{\partial C}{\partial x}=KC_0, \tag{7}$$

where C_0 is the concentration of nontrapped deuterium at the surface and K is the thermal desorption rate constant. The boundary condition for nontrapped deuterium at the layer interface, with a continuous flux E into the silicon substrate, can be written as

$$D_f\frac{\partial C}{\partial x}=-E. \tag{8}$$

This flux was very small and observed only at high temperatures in silicon doped samples.

B. Computational method

The Eqs. (1)–(8) were solved numerically by a finite difference method. In this method the solution domain is discretized and the computation nodes form a rectangular grid in space and time. Both the space and time grids are taken to be nonuniform to maximize the accuracy and minimize the computational effort. The nonuniform grid excludes the Duford-Frankel method.[18] For discretization in the space domain, we use the second-order finite difference scheme for the second space derivative in Eq. (1)

$$\frac{\partial^2 C_i}{\partial x^2}\approx\frac{2C_{i-1}}{\Delta x_i(\Delta x_i+\Delta x_{i+1})}-\frac{2C_i}{\Delta x_i\Delta x_{i+1}}+\frac{2C_{i+1}}{\Delta x_{i+1}(\Delta x_i+\Delta x_{i+1})}, \tag{9}$$

where $\Delta x_i=x_i-x_{i-1}$ is the spacing of the nodes in the depth direction. The numerical solution of Eq. (1) by the explicit Euler method[18] demands maximum time steps to be proportional to $\min(\Delta x)^2/D$. The minimum value of Δx was 1 nm, and the maximum diffusion coefficient about 500 nm^2/s. This means that for a total diffusion time of 2000 s, about 10^6 iterations are needed to complete a solution. Clearly a

faster method is needed for analyzing large number of experimental diffusion profiles. Denoting the discretized right-hand side of Eq. (1) by $L(C,C_t)$, the second-order Crank-Nicholson method[18] for discretization in time domain is

$$\frac{C^{n+1}-C^n}{\Delta t}=L\left[\frac{C^{n+1}+C^n}{2},\frac{C_t^{n+1}+C_t^n}{2}\right], \tag{10}$$

where n is the index referring to the time step and Δt is the length of the time step. The pointwise error estimate for the diffusion term in Eq. (1) can be derived by applying the Crank-Nicholson method to linear diffusion equations. When detrapping and trapping are neglected, the error estimate per unit time becomes[18]

$$\frac{\partial C}{\partial t}-D_f\frac{\partial^2 C}{\partial x^2}\approx\frac{(\Delta t)^2}{12}\frac{\partial^3 C}{\partial t^3}+\frac{D_f}{12}\left[(\Delta x)^2\frac{\partial^4 C}{\partial x^4}\right], \tag{11}$$

where Δx is the node separation in a uniform space grid. This estimate holds quite well also for a slowly changing nonuniform grid. The error resulting from the space discretization was minimized by evaluating the fourth space derivative of the experimental deuterium depth profiles and choosing the node separation in the depth coordinate by keeping the product in the square brackets of Eq. (11) constant, i.e.,

$$(\Delta x)^2\frac{\partial^4 C}{\partial x^4}=\text{const.} \tag{12}$$

The node separation at the surface, where the concentration profile is curved, was chosen to be 1 nm. Deeper in the substrate the node separation could be increased and was between 10 and 30 nm at the deep end of the deuterium profile.

The error due to discretization in time domain is given in Eq. (11). The time step Δt could be increased in the course of computation. This was done by approximating the third derivative of C with respect to time by Lagrange interpolation, using data from four previous time steps. The first four time steps were computed using small constant time steps. The size of the time step is then calculated using Eq. (11)

$$\Delta t=\sqrt{\frac{12E_{max}}{T[\partial^3 C/\partial t^3]_{max}}}, \tag{13}$$

where E_{max} is the error tolerance and T the total diffusion time. In this way the initial time step of 0.1 s increased during calculations to about 1 s, reducing the total computational effort compared to the Euler method by about two orders of magnitude. This method was used to solve numerically Eqs. (1)–(8). The fitted parameters were the ones given in Eqs. (1) and (2), namely, the diffusion coefficient, detrapping and retrapping coefficients, and the trapping density. The thermal desorption coefficient in Eq. (7) and in some cases also the term describing flux of deuterium into the silicon substrate in Eq. (8), were fitting parameters. These fitting parameters were then used to calculate the theoretical depth profiles of nontrapped and trapped deuterium. Their sum was compared with the experimental profiles. New parameter values were given and the iteration process continued until a satisfactory fit was obtained.

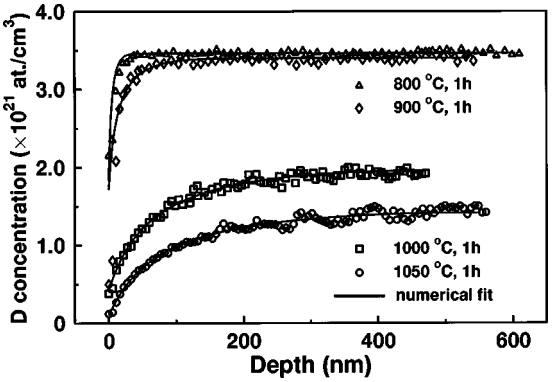

FIG. 1. Experimental concentration profiles of deuterium obtained after isochronal annealing of DLC samples not containing Si, together with numerical fits. The as-deposited profile for the pure DLC film is not presented because it overlaps with the profile of the sample annealed at 800 °C, except in the vicinity of the surface.

IV. RESULTS AND DISCUSSION

Deuterium concentration profiles together with the numerical fits for isochronal annealing at different temperatures for carbon films without Si and with Si content of 6 at. % are shown in Figs. 1, and 2, respectively. The agreement between the experimental SIMS profiles and the theoretical fits is very good in both figures. Figure 3 presents the concentration profiles and numerical fits for carbon films not containing Si and annealed at 1000 °C for 1, 2, and 4 h. The fitting parameters for the diffusion model [Eqs. (1), (2), and (7)] were obtained to be the same within error limits, indicating a steady-state diffusion. No in diffusion of deuterium into the Si substrate was observed.

As can be seen in Figs. 1–3, the decrease in the deuterium concentration occurs not only at the near surface region but in the bulk as well. This effect cannot be described by taking into account diffusion process only, but trapping and detrapping of D are needed to be considered as well. The loss of D

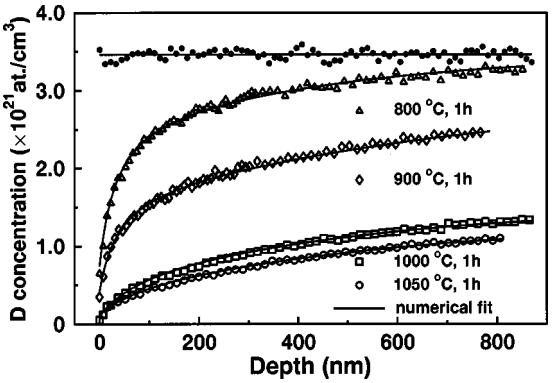

FIG. 2. Experimental concentration profiles of deuterium obtained after isochronal annealing of DLC samples with a Si concentration of 6 at. %, together with numerical fits. The dots show the as-deposited deuterium profile.

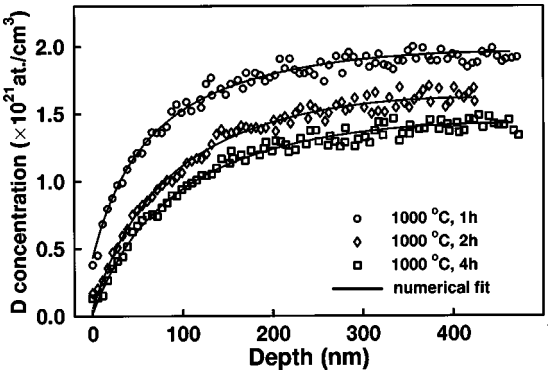

FIG. 3. Experimental concentration profiles of deuterium obtained after annealing of Si-free DLC samples at 1000 °C for 1, 2, and 4 h, together with numerical fits. Deuterium concentration in the as-deposited sample was 3.5×10^{21} at. %/cm^3.

at the surface region occurs due to the thermal desorption of D atoms to vacuum. This results in a concentration gradient and initiates deuterium diffusion from the bulk towards the surface. The lowering of the D concentration level deep inside the layer occurs because the diffusion is trap controlled, i.e., most of D atoms are bonded or trapped to carbon and silicon atoms. Once emitted or detrapped, a D atom will migrate fast until it is trapped again. The trapping density is constant in the layer, thus in a region where the D concentration is large, there is only a small amount of empty traps. Consequently, when a D atom is detrapped in this region, it spends a longer time in a mobile configuration than a D atom in a region of a low D and thus high empty trap concentration. This is the reason for the apparent concentration or time dependency for the D diffusion seen in Fig. 3, i.e., after annealing for 1 h about 50% of the initial D amount was removed, after which the process seems to be much slower.

The deuterium retention as a function of temperature in DLC samples is presented in Fig. 4. The D loss from the samples increases when Si is incorporated to the carbon network. The highest D release occurs in samples with Si content of 15 at. %, whereas in films with Si concentration of 33 at. % it is again lower. To describe the complicated matter of D retention in these materials, we have to look at the interplay of the diffusivity, trapping, and detrapping of D.

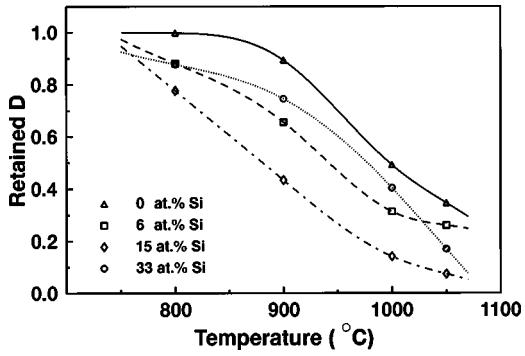

FIG. 4. Amount of retained deuterium as a function of temperature in samples with different Si concentrations. The lines are drawn to guide the eye.

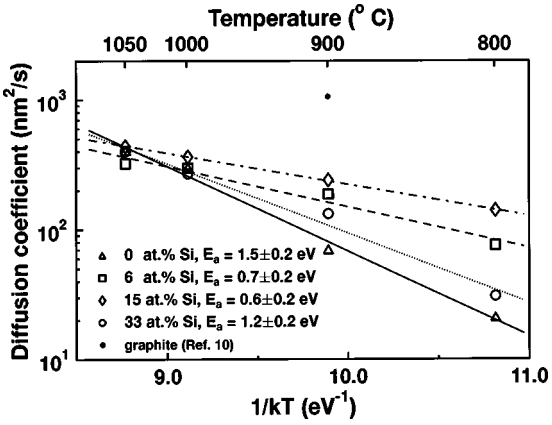

FIG. 5. Arrhenius plot for the diffusion coefficient of nontrapped deuterium. Shown are the natural logarithms of the diffusion coefficients vs 1/kT. The lines are the fits to the experimental data.

The Arrhenius plots in Fig. 5 show that the activation energy for the diffusion of nontrapped D in pure DLC is about 1.5 eV. When Si concentration increases, the activation energy decreases to 0.7 and 0.6 eV for 6 and 15 at. % of Si, respectively. To understand the decrease in the framework of the incorporation of silicon atoms into the amorphous carbon structure, we compare our results with the activation energy of 0.3 eV obtained by Branz[19] for the diffusion of nontrapped hydrogen in amorphous Si. Silicon atoms seem to decrease the energy barrier for diffusion jumps of hydrogen atoms. In pure DLC the atom density is about 1.2×10^{23} at. %/cm^3 while in Si it is about 5.0×10^{22} at. %/cm^3. A high density of substrate atoms probably decreases the diffusivity. The further increase of the activation energy to 1.2 eV (Fig. 5) for DLC with 33 at. % of Si can be interpreted to reflect the changes in the bond structure that takes place with the increasing Si amount.[17] The number of the Si-C bonds in similar Si-doped DLC films was measured with the x-ray photoelectron spectroscopy.[20] The relative amount of the Si-C bonds in samples with the Si content of 6 and 15 at. %, was quite low, 2 and 8%, respectively, while in the samples with Si content of 33 at. % it was drastically increased to 45%. Moreover, the Si-C network (Si content of 33 at. %) is stable under thermal treatment and energetic heavy-ion irradiation.[17] The activation energy for hydrogen diffusion in SiC has been found to be as high as 3.5 eV.[21] Since different materials have been used in this paper, no definite conclusions can be drawn. However, the trend of the increasing activation energy in materials with a high Si-C bond fraction is remarkable. The activation energy $E_a=1.5\pm0.2$ eV obtained for pure DLC films is different from the result $E_a=2.9\pm0.1$ eV reported previously by us for D implanted samples.[12] This is explained by the fact that a different model was used to fit the experimental profiles. In Ref. 12, the trapped D was assumed to be an analytical function of the total D concentration, which simplified the diffusion calculations for implanted D. By employing the current calculation procedure, we obtained a concentration distribution that matches very well with the previous SIMS data[12] (see Fig. 6) observed for the D implanted sample annealed at

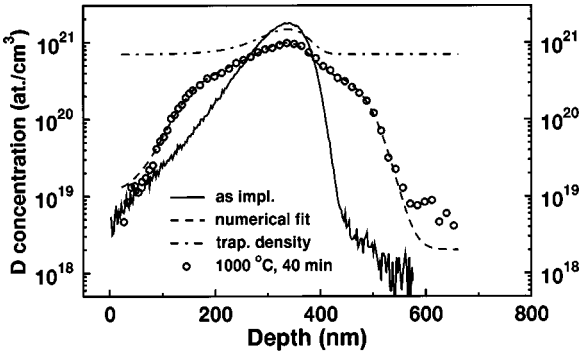

FIG. 6. Experimental concentration profiles of deuterium obtained in Ref. 12 after implantation (solid line) and annealing at 1000 °C for 40 min (open circles). The dashed line is a numerical fit obtained by the diffusion model presented in this paper. The dot-dashed line shows the total trapping density.

1000 °C for 40 min. The deduced diffusion coefficient of about 300 nm^2/s is very close to the ones shown in Fig. 5 for D co-deposited samples annealed at 1000 °C.

For the D implanted samples, the trapping density (the dot-dashed line in Fig. 6) was assumed to contain two parts, namely, a constant value through the whole film and the second term proportional to the implanted D concentration. This plausible choice of trapping density explains the experimentally observed kinks present at the distribution at about 200 and 400 nm.

The density of D traps obtained in fitting processes for outdiffusion of D from Si-doped and Si-free DLC films is illustrated in Fig. 7. It increases with the increase of the Si content in the Si-DLC samples. However, the value of trapping density for DLC films not containing Si is higher than for coatings with the Si content of 15 at. % and lower than for the films with Si concentration of 33 at. %. We suppose that the reason for the decrease of the number of D traps as a function of temperature is the removing of carbon and silicon dangling bonds due to the formation of bonds with other carbon and silicon atoms, which takes place when the total D concentration decreases with increasing temperature.

Numerical fittings to the experimental profiles were obtained to depend on the ratio of the detrapping and trapping coefficients but not on their absolute values. The ratio is defined as $Frac=\Sigma_D/\Sigma_T$ and presented in Fig. 8. *Frac* is higher in Si-DLC than in Si-free DLC. This means that the detrapping rate is higher and/or trapping rate lower in the Si-DLC films than in the DLC films without Si. During the deposition process, D forms bonds with Si atoms rather than with C atoms.[22] In a diatomic molecule, lower energy is needed to break the Si-H bond than the C-H bond.[23] This leads to the enhanced detrapping process in Si-doped films due to the presence of a higher amount of the Si-D bonds, which are easier to break than the C-D bonds. Detrapping takes place when an energy barrier is overcome and therefore the process is temperature dependent and follows the Arrhenius form.[19] Activation energies for *Frac* in Si containing films are lower than in pure DLC coatings. However, it increases as a function of Si content and in samples with Si concentration of 33 at. %, it has a value of 1.3 eV. For a qualitative comparison only, the calculated activation energy for the trap-controlled H diffusion in *a*-Si:H is 1.4 eV.[19]

The surface coefficient as a function of temperature is shown in Fig. 9. It increases with the rising temperature and goes down again after the maximum value at about 1000 °C. It is not easy to draw any definite conclusions from a general

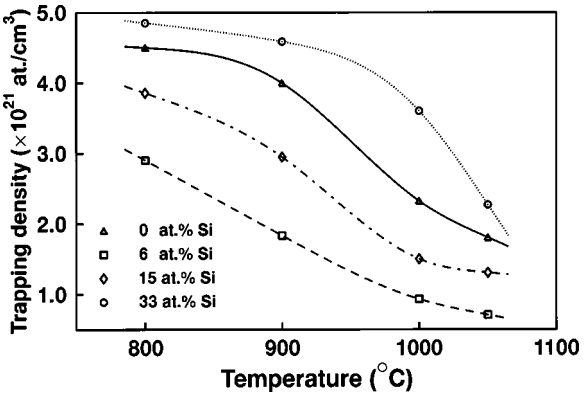

FIG. 7. Trapping density as a function of temperature in samples with different Si concentrations. The lines are drawn to guide the eye.

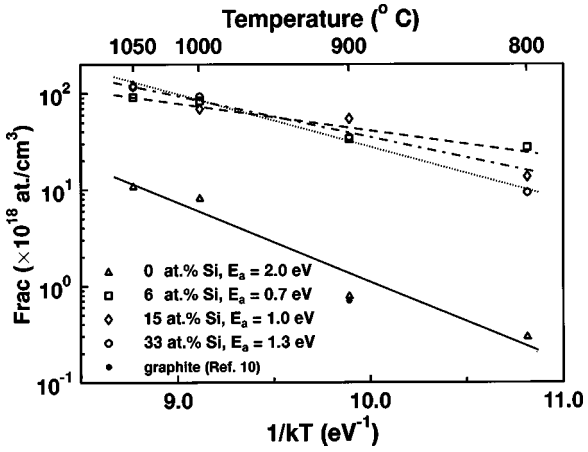

FIG. 8. *Frac*, i.e., ratio of detrapping and trapping coefficients, as a function of temperature in samples with different Si concentrations. The lines are the fits to the experimental data.

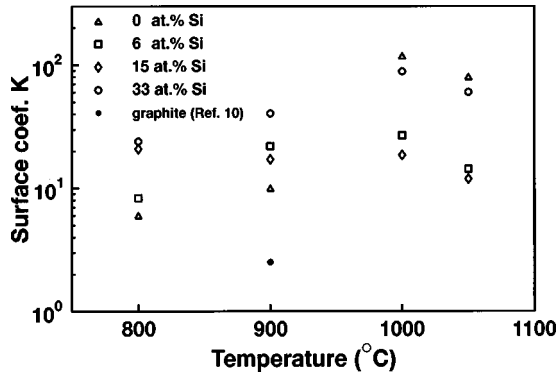

FIG. 9. Surface coefficient as a function of temperature in samples with different Si concentrations.

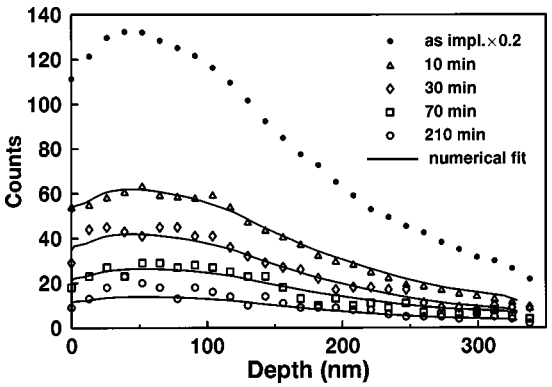

FIG. 10. Experimental concentration profiles of hydrogen obtained by B. Tsuchiya and K. Morita (Ref. 10) after annealing of graphite samples at 900 °C for 10, 30, 70, and 210 min. The lines show the numerical fits obtained by the diffusion model presented in this paper.

trend because SIMS, due to high sputtering rates used in the analysis, and TOF-ERDA are not sensitive enough at the surface.

To test further the current model and compare our results with those presented for graphite, we fitted the model to the implanted hydrogen profiles reported by Tsuchiya and Morita.[10] The profiles were obtained by a 5-keV H_2 implantation to a saturation dose at room temperature. The H profiles were obtained in measurements done with a 1.5-MeV He^+ elastic recoil detection method. Experimental profiles together with the numerical fits are presented in Fig. 10. The annealing temperature was 900 °C for all profiles and the annealing time 10, 30, 70, and 210 min. Each numerical fit in the figure is calculated using the same diffusion coefficient, trapping density, detrapping/trapping ratio, and surface boundary coefficient, see Eqs. (1)–(8). The only parameter that was different for each calculation was the boundary condition coefficient for the hydrogen flux into the bulk graphite, see Eq. (8). It had the values of 15, 3, 0.1, and 0.1×10^{-7} at. %/s cm^2 for the 10, 30, 70, and 210-min annealing, respectively. The H flux into the graphite is thus higher in the beginning of the annealing when the H concentration is high but decreases with the annealing time and H concentration. In the implanted samples the H trapping density was observed to vary over the implanted region. The implantation is always accompanied by a defect formation and a realistic defect distribution could be obtained by either SRIM (Ref. 15) or molecular-dynamics calculations. Because the resolution of the ERD system is not known, it was not possible to use the calculations to obtain the damage distribution. Instead it was sufficient to assume that it has the shape of the as implanted H profile. The best numerical fits shown in Fig. 10 were obtained when the damage distributions were deduced by multiplying the H concentration distribution with 0.11. To estimate the actual concentration of H traps, we need to know the implanted H concentration. The saturation concentration of H has been reported to be 30–40 at. %.[24,25] The H trap density would then be about 3–4 at. %. This estimate is in agreement with the current value obtained for the trapping density of D in the Si-free DLC at 900 °C, see Fig. 7. The diffusion coefficient was observed to be much higher for nontrapped H in graphite than in DLC (Fig. 5) as could be expected.

A noteworthy result is that the detrapping/trapping ratio in the H implanted samples was observed to be the same as the ratio for the D out diffusion from Si-free DLC films, Fig. 8. The major difference in the diffusion behavior of hydrogen in DLC and graphite is thus due to the evident difference in the diffusion coefficient of nontrapped hydrogen.

V. CONCLUSIONS

Annealing behavior of deuterium in co-deposited Si-free and Si-DLC samples was studied. The obtained depth profiles have been fitted with a model that takes into account diffusion of nontrapped D atoms, thermal detrapping, and trapping. The diffusion coefficients exhibit a good Arrhenius behavior with activation energies of 1.5 ± 0.2, 0.7 ± 0.2, 0.6 ± 0.2, and 1.2 ± 0.2 eV for the samples containing 0, 6, 15, and 33 at. % of Si, respectively. The presented model can be used to explain the annealing behavior of hydrogen isotopes in DLC films, graphite, Si-free, and Si-doped carbon based materials, and in implanted and co-deposited films.

ACKNOWLEDGMENTS

This work was supported in part by the Academy of Finland (Project No. 45090130) and by the Association Euratom TEKES. Authors want to thank J. Kolehmainen and J. Partanen (DIARC Technology Inc.) for sample preparation. The electron microscope unit of the University of Helsinki is acknowledged for giving the scanning electron microscope to our disposal.

*Corresponding author. FAX: +358 9 19140042, Email address: elizaveta.vainonen@helsinki.fi

†Permanent address: Technical Research Center of Finland, Chemical Technology, P.O. Box 1404, FIN-02044 VTT, Finland.

[1] S. M. Sze, *Physics of Semiconductor Devices* (Wiley, New York, 1981), pp. 790–838.

[2] S. A. Kajihara, A. Antonelli, J. Bernholc, and R. Carr, Phys. Rev. Lett. **66**, 2010 (1991).

[3] M. I. Landstrass and K. V. Ravi, Appl. Phys. Lett. **55**, 1391 (1989).

[4] M. I. Landstrass and K. V. Ravi, Appl. Phys. Lett. **55**, 975 (1989).

[5] M. Balden, J. Roth, and C. H. Wu, J. Nucl. Mater. **258-263**, 740 (1998).

[6] W. R. Wampler, B. L. Doyle, R. A. Causey, and K. L. Wilson, J. Nucl. Mater. **176&177**, 983 (1990).

[7] J. W. Davis and A. A. Haasz, J. Nucl. Mater. **183**, 229 (1991).

[8] S. Chiu and A. A. Haasz, J. Nucl. Mater. **196-198**, 972 (1992).

[9] Y. Muto and K. Morita, J. Nucl. Mater. **223**, 262 (1995).

[10] B. Tsuchiya and K. Morita, J. Nucl. Mater. **220-222**, 836 (1995).

[11] E. Vainonen, J. Likonen, T. Ahlgren, P. Haussalo, J. Keinonen, and C. H. Wu, J. Appl. Phys. **82**, 3791 (1997).

[12] T. Ahlgren, E. Vainonen, J. Likonen, and J. Keinonen, Phys. Rev.

B **57**, 9723 (1998).
[13] J. Saarilahti and E. Rauhala, Nucl. Instrum. Methods Phys. Res. B **64**, 734 (1992).
[14] J. F. Ziegler, J. P. Biersack, and U. Littmark, in *The Stopping and Range of Ions in Solids* (Pergamon, New York, 1985), Vol. 1.
[15] J. F. Ziegler and J. P. Biersack, SRIM-96 computer code (private communication).
[16] J. Jokinen, J. Keinonen, P. Tikkanen, A. Kuronen, T. Ahlgren, and K. Nordlund, Nucl. Instrum. Methods Phys. Res. B **119**, 533 (1996).
[17] L. Khriachtchev, E. Vainonen-Ahlgren, T. Sajavaara, T. Ahlgren, and J. Keinonen, J. Appl. Phys. **88**, 2118 (2000).
[18] J. H. Ferziger, *Numerical Methods for Engineering Application* (Wiley, New York, 1981).
[19] H. M. Branz, Phys. Rev. B **60**, 7725 (1999).
[20] Research Report No. VAL62-6016, VTT Manufacturing Technology, Espoo, Finland, 1996.
[21] M. K. Linnarsson, J. P. Doyle, and B. G. Svensson, in *Materials of III-Nitride, SiC and Diamond Materials for Electronic Devices Symposium* (Mater. Res. Soc., Pittsburgh, PA, 1996), p. 625.
[22] E. Vainonen-Ahlgren, T. Sajavaara, W. Rydman, T. Ahlgren, K. Nordlund, and J. Keinonen in *NATO Advanced Research Workshop Series* (Kluwer, Dordrecht, Netherlands) (unpublished).
[23] *CRC Handbook of Chemistry and Physics*, edited by D. R. Lidy (CRC Press, Boca Raton, Florida, 1996).
[24] J. Roth, B. M. U. Scherzer, R. S. Blewer, D. K. Brice, S. T. Picraux, and W. R. Wampler, J. Nucl. Mater. **93&94**, 601 (1980).
[25] B. L. Doyle, W. R. Wampler, and D. K. Brice, J. Nucl. Mater. **103&104**, 513 (1981).